# Recent Developments in Near-Surface Imaging using DAS and NHERI@UTexas Mobile Shakers

**Brady R. Cox, Ph.D., P.E.**
Professor, Civil Engineering, Utah State University
**Peter Hubbard, Ph.D.**
Lead Engineer, FiberSense

also with contributions from the work of
**Joseph Vantassel, Ph.D.**
Assistant Professor, Civil Engineering, Virginia Tech
**Michael Yust, Ph.D.**
Slate Geotechnical Consultants

NHERI@UTexas Virtual Workshop on Potential Opportunities for NSF Research in Hawaii
14 December 2022

UtahState University
CIVIL AND ENVIRONMENTAL ENGINEERING

LARGE MOBILE SHAKERS
NHERI@UTexas

NSF

# Distributed Acoustic Sensing (DAS) – What is it?

## Sensing axial strain ($\varepsilon_a$) with laser interferometry (light phase change)

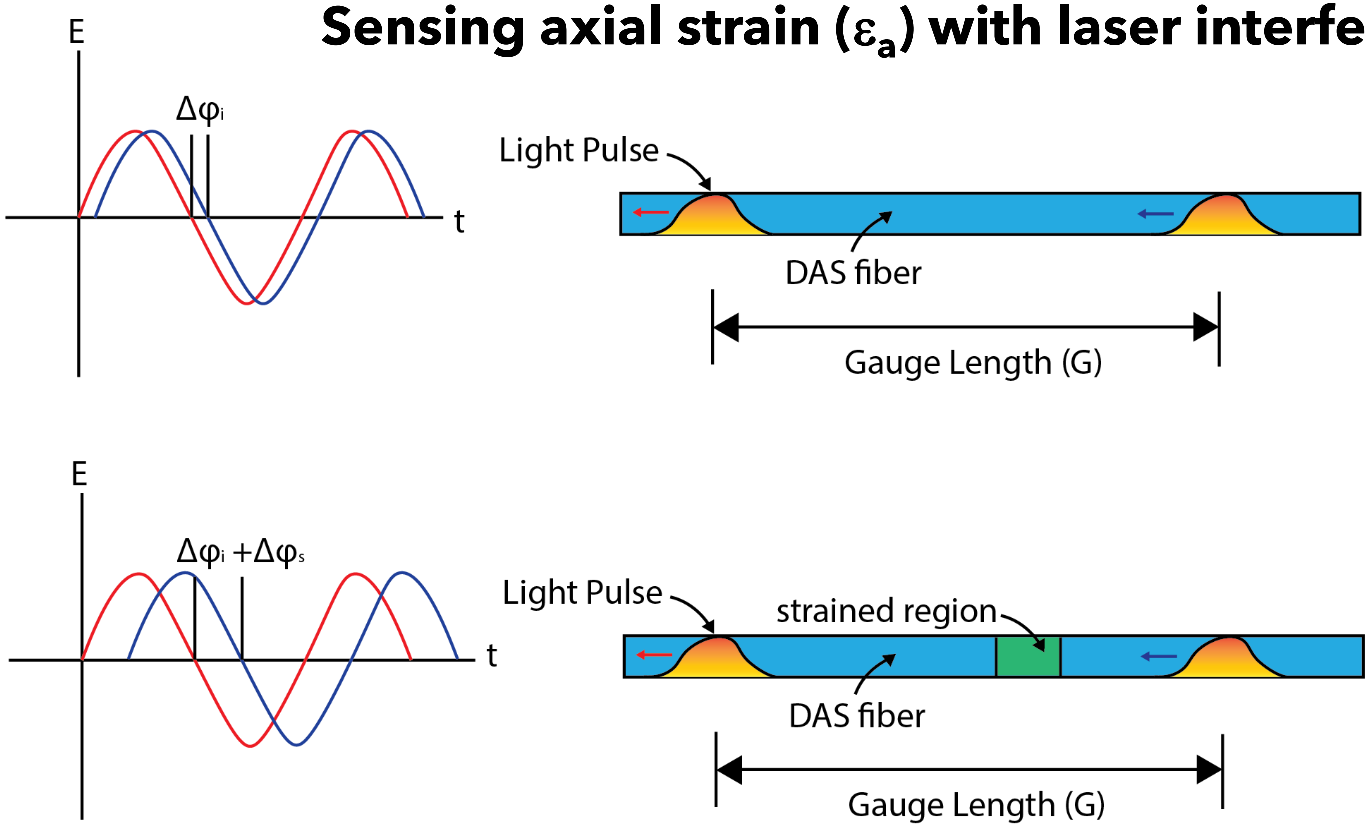

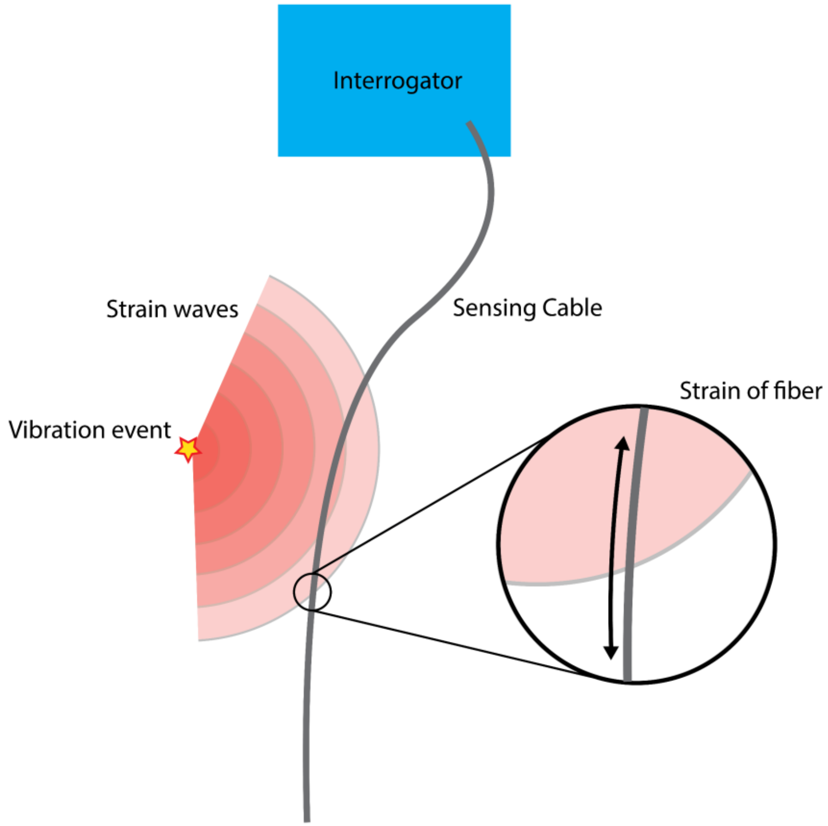

Change in length of fiber section: $\Delta u = \frac{\lambda}{2\pi}\frac{1}{n\xi}\frac{\Delta\varphi}{2}$, $\quad \varepsilon_a = \frac{\Delta u}{G}$

Where $\lambda$ is the optical wavelength of the laser, $\eta$ is the group refractive index of the fiber, and $\xi$ is the photoelastic scaling factor for axial strain in the fiber

# Why DAS?

Ability to sense seismic wavefields over **large spatial scales (e.g., kilometers)** while still maintaining **high spatial resolution (e.g., 1-m channel separation)**

Interrogator Unit (IU)

OptaSense®
A QINETIQ company

Fiber Optic Cable

**LARGE MOBILE SHAKERS**
NHERI@UTexas

Thumper

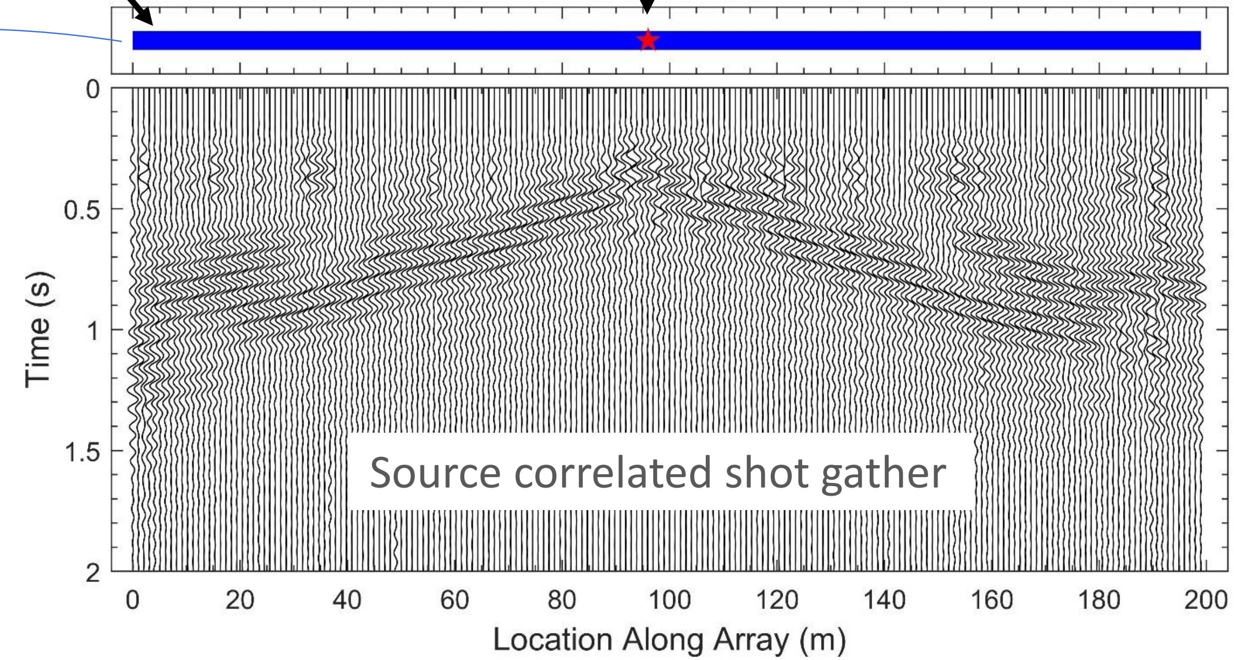

Source correlated shot gather

- Sample rate up to 100 kHz
- Selectable gauge length (2m to 34m)
- 1-m channel/trace separation

# Recent Studies/Publications using DAS and NHERI@UTexas Mobile Shakers

1. Hubbard, P.G., Vantassel, J.P., Cox, B.R., Rector, J.W., Yust, M., Soga, K. (2022). "**Quantifying the Surface Strain Field Induced by Active Sources with Distributed Acoustic Sensing: Theory and Practice**," *Sensors*, 22(12):4589. https://doi.org/10.3390/s22124589.

   Geophones vs. DAS

2. Vantassel, J.P., Cox, B.R., Hubbard, P.G., Yust, M. (2022). "**Extracting High-Resolution, Multi-Mode Surface Wave Dispersion Data from Distributed Acoustic Sensing Measurements using the Multichannel Analysis of Surface Waves**," *Journal of Applied Geophysics*, https://doi.org/10.1016/j.jappgeo.2022.104776.

   DAS for 1D MASW

3. Yust, M.B.S., Cox, B.R., Vantassel, J.P., Hubbard, P.G. (2023 submitted). "**DAS for 2D MASW Imaging: A Case Study on the Benefits of Flexible Sub-Array Processing**," (submitted to *Near Surface Geophysics*).

   DAS for Pseudo-2D MASW

4. Yust, M.B.S., Cox, B.R., Vantassel, J.P., Hubbard, P.G., Boehm, C., Krischer, L. (2023 in preparation). "**Near-Surface 2D Imaging via FWI of DAS Data: An Examination on the Impacts of FWI Starting Model**," (to be submitted to a special issue on Seismic Full-Waveform Imaging and Inversion across Scales in *Geosciences*).

   DAS for True 2D Imaging via FWI

# Multi-Directional Shaking with DAS at Hornsby Bend

LARGE MOBILE SHAKERS
NHERI@UTexas

3D shaking capability allows for controllable wavefield polarizations

TRex

DESIGNSAFE

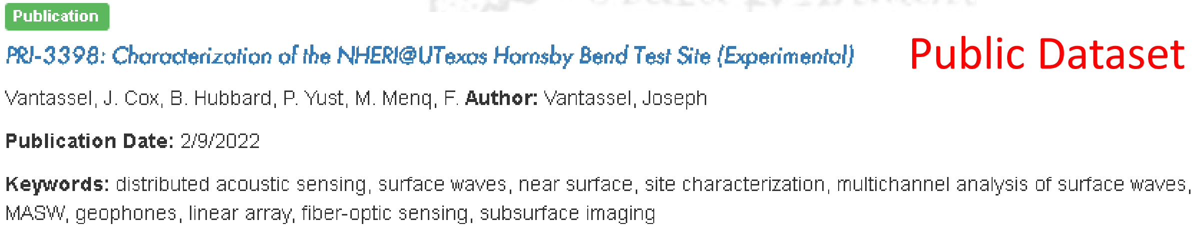

Publication

*PRJ-3398: Characterization of the NHERI@UTexas Hornsby Bend Test Site (Experimental)*

Public Dataset

Vantassel, J. Cox, B. Hubbard, P. Yust, M. Menq, F. **Author:** Vantassel, Joseph

**Publication Date:** 2/9/2022

**Keywords:** distributed acoustic sensing, surface waves, near surface, site characterization, multichannel analysis of surface waves, MASW, geophones, linear array, fiber-optic sensing, subsurface imaging

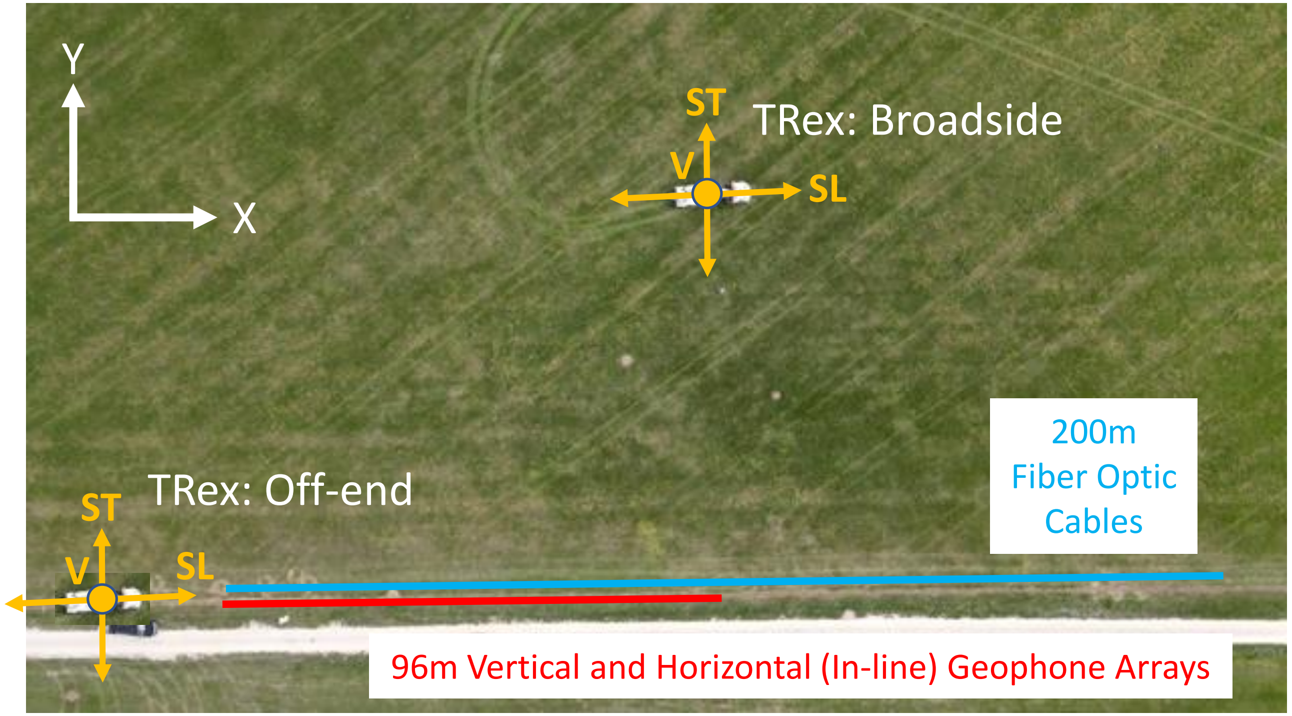

200m Fiber Optic Cables

96m Vertical and Horizontal (In-line) Geophone Arrays

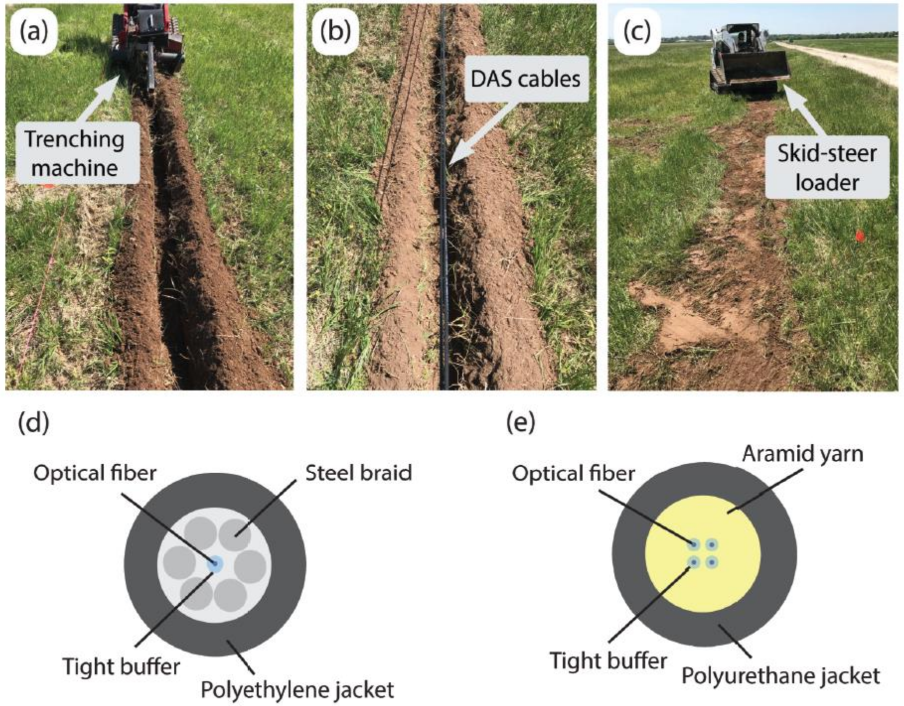

Nanzee – strain sensing

AFL – tight buffered

# Experimental DAS Reception Patterns

LARGE MOBILE SHAKERS
NHERI@UTexas

3D shaking capability allows for controllable wavefield polarizations

TRex

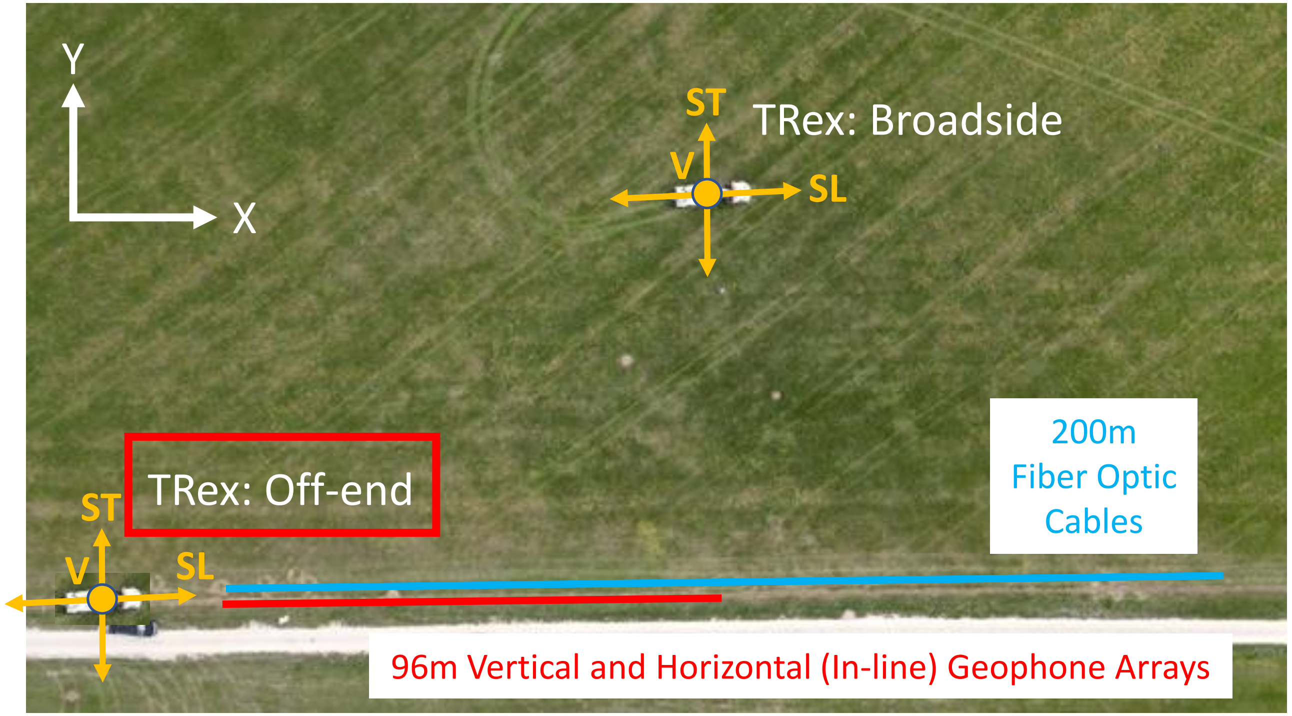

MASW, Refraction, FWI

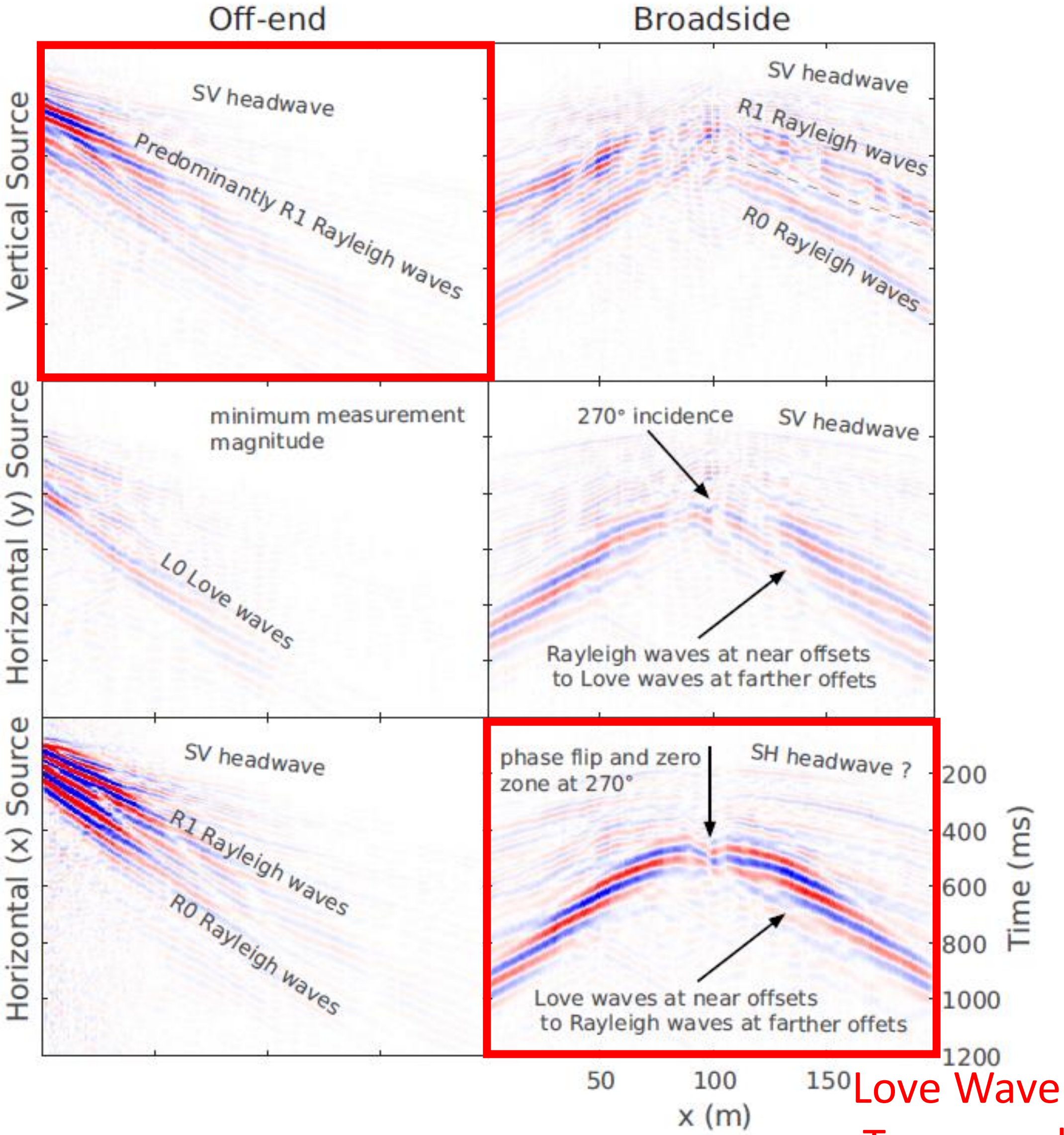

Love Wave Tomography

# MASW: Geophones vs. DAS - waveforms

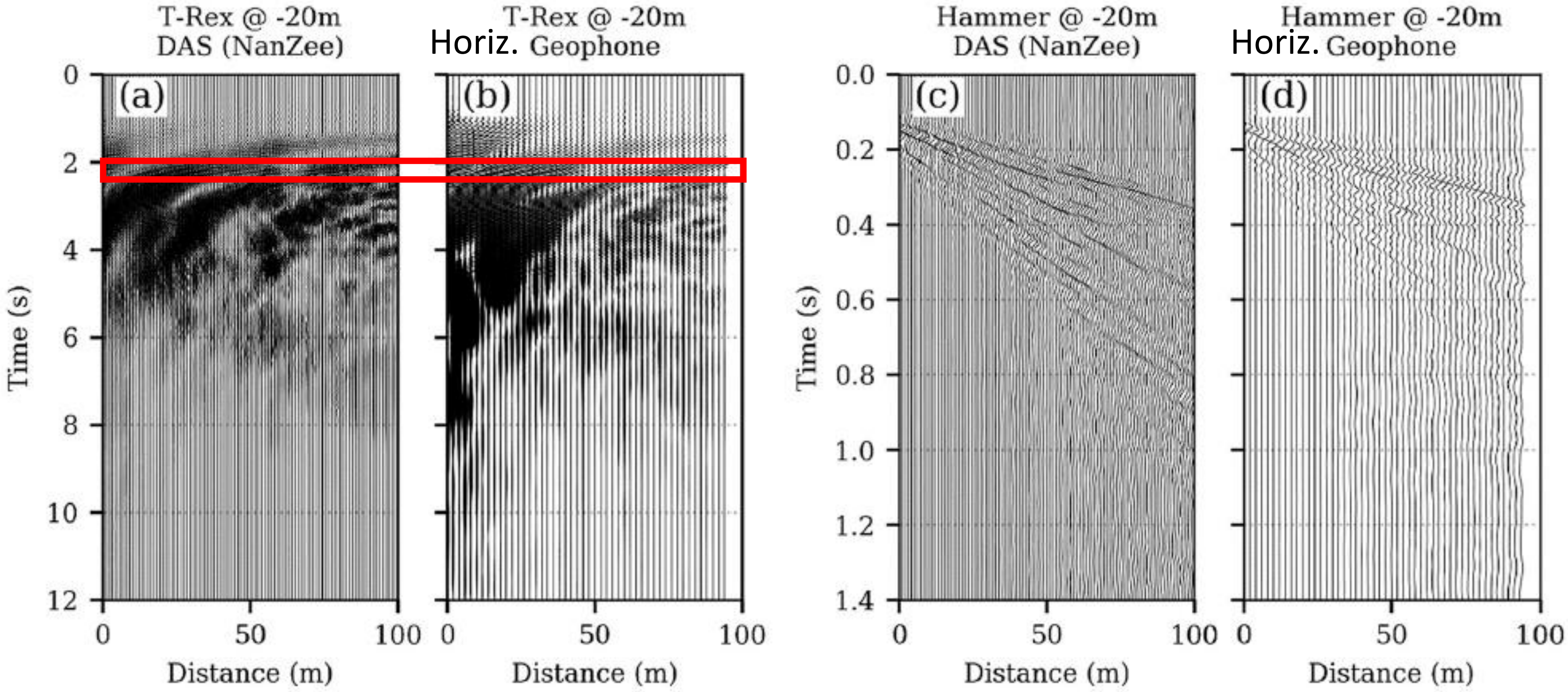

2m gauge length
1m ch. spacing
Horiz. axial strain

2m geo. spacing
Horiz. particle vel.

2m gauge length
1m ch. spacing
Horiz. axial strain

2m geo. spacing
Horiz. particle vel.

# MASW: Geophones vs. DAS - waveforms

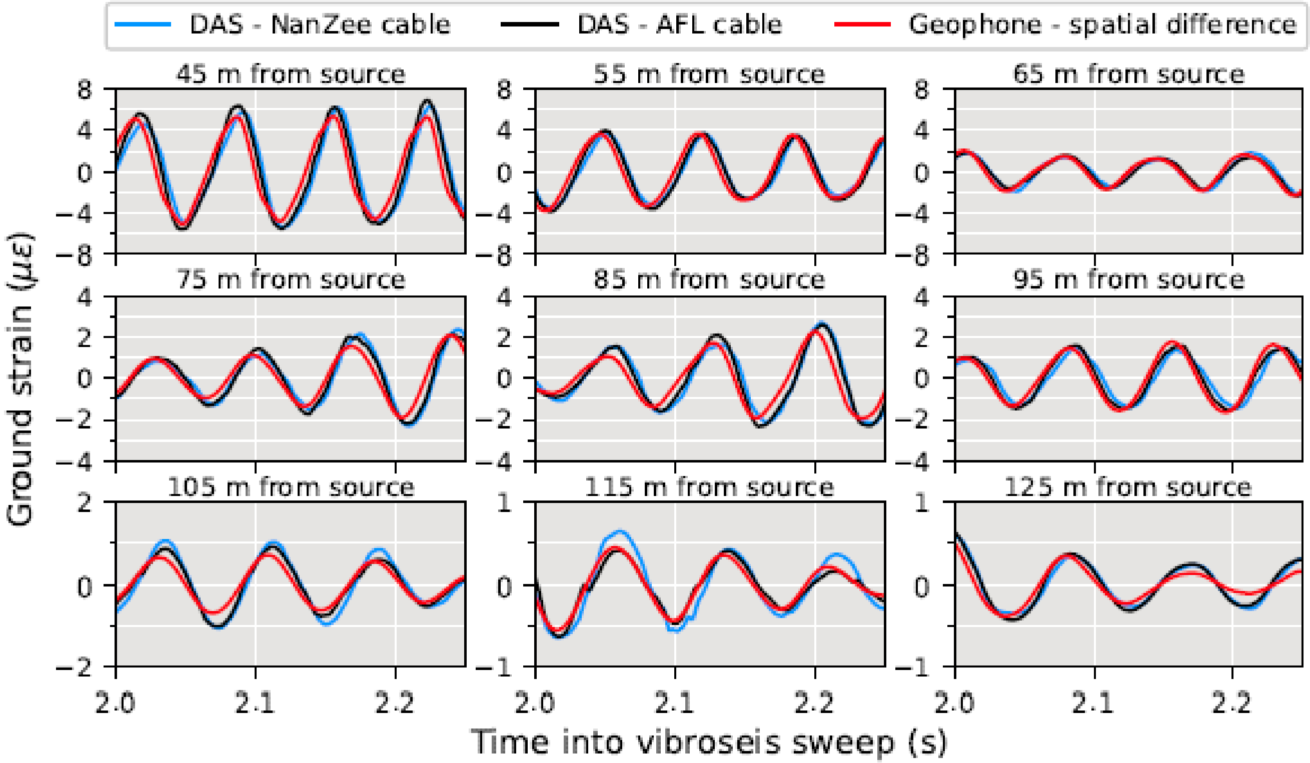

“DAS measures ground deformation quantitatively with both amplitude and phase that agree with measurements made by geophones.” Hubbard et al. (2022)

# Importance of Wavelength & Loading Direction when Comparing DAS vs. Geophone Waveforms

Response due to wavelength

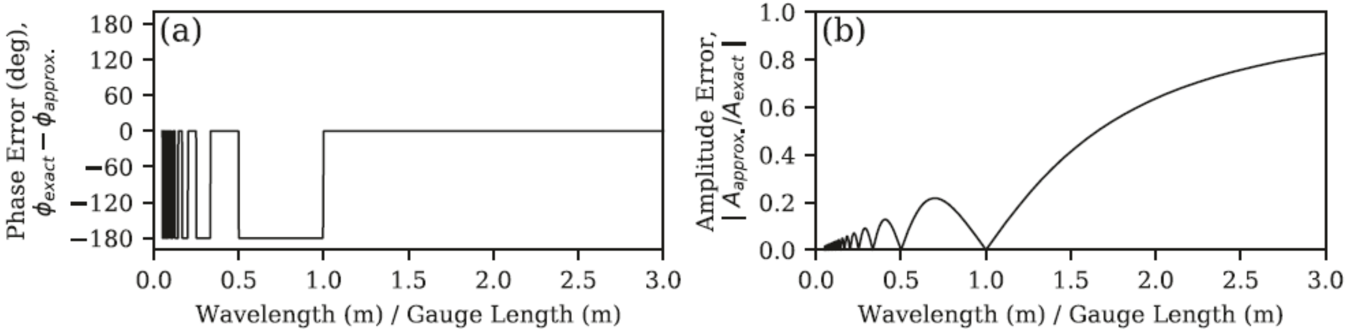

λ > g for accurate phase

λ > 3*g for accurate amp.

- DAS spatial transfer function due to gauge length can be described as:

$$\mathbb{G}(k_a) = \mathcal{F}\left\{\frac{1}{g}\Pi\left(\frac{x}{g}\right)\right\} = \frac{\sin(\pi k_a g)}{\pi k_a g}$$

Response due to loading direction

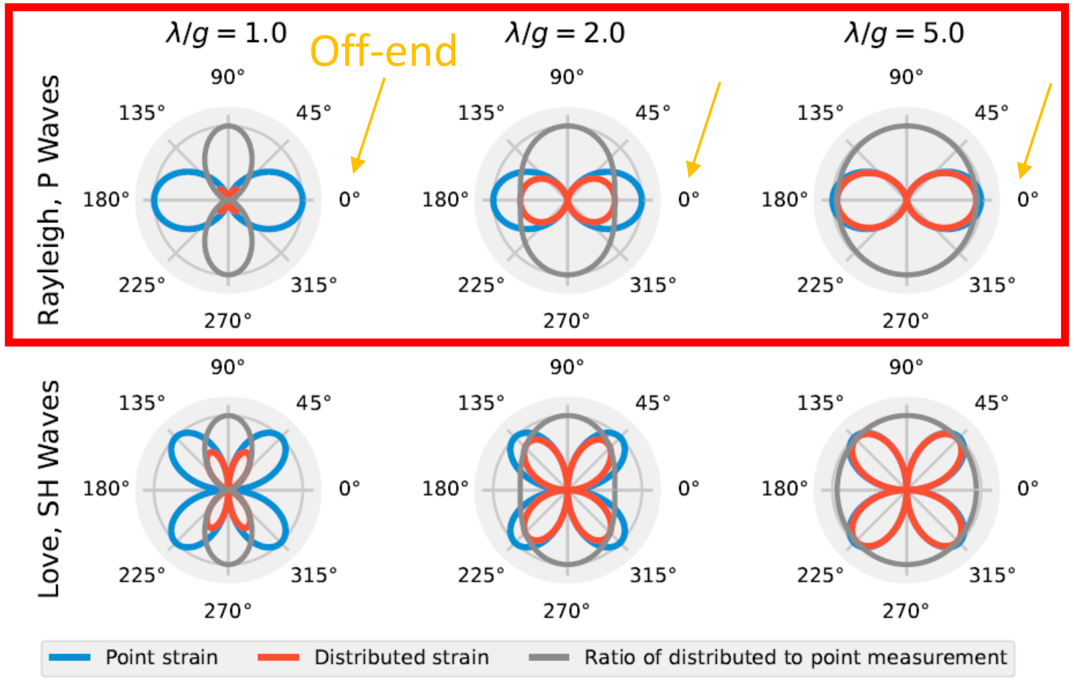

**Figure 2.** Radial reception patterns for pointwise strain and ideal distributed sensor-measured strain for wavelength to gauge length ratios ($\lambda/g$) of 1, 2, and 5 for Rayleigh, P, Love, and SH waves. The patterns are plotted such that the maximum pointwise strain value is 1. In addition, the ratios of theoretical distributed strains and pointwise strains are shown as a function of angle in the horizontal plane ($\theta$), which approaches unity for all wave types and angles as $\lambda/g$ increases.

# MASW: Geophones vs. DAS – dispersion data

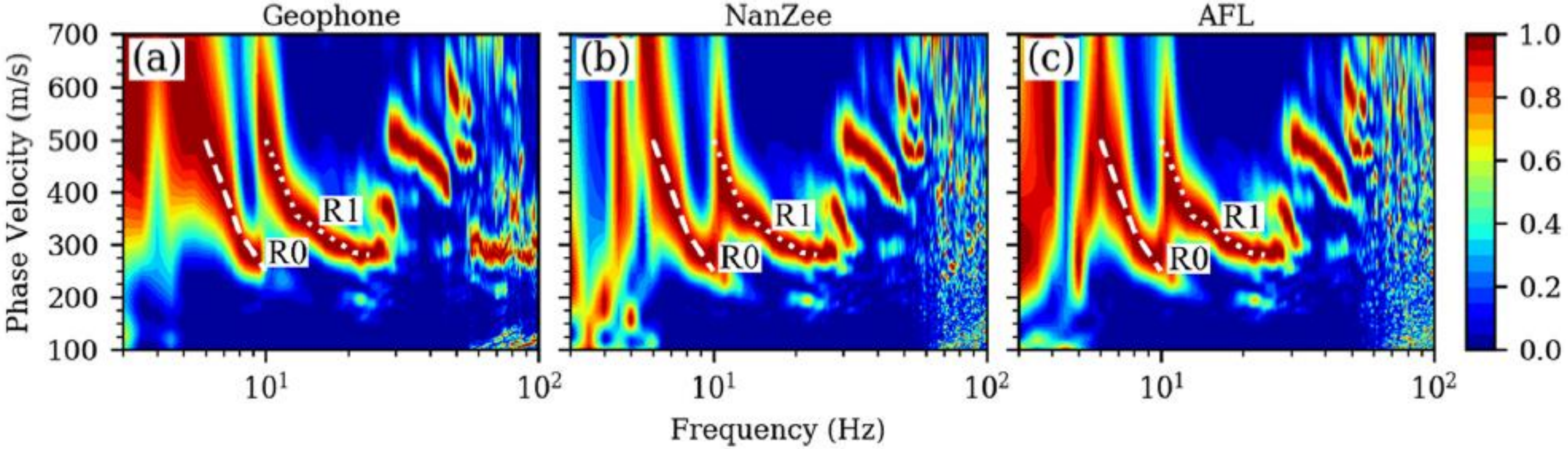

**Fig. 5.** Comparison of surface wave dispersion images from three vertical T-Rex chirps stacked in the time domain at the source location of −40 m as derived from

2m geophone spacing
Horiz. particle vel.

2m gauge length
1m channel spacing
Horiz. axial strain

# MASW: Geophones vs. DAS – dispersion data Importance of Gauge Length and Wavelength

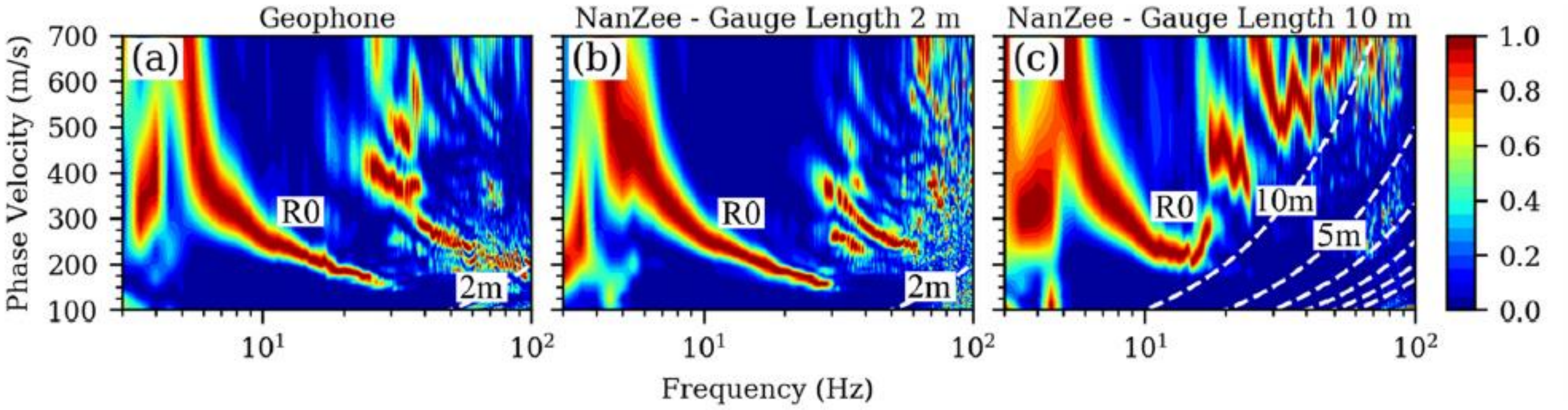

**Fig. 6.** Comparison of surface wave dispersion images from three in-line T-Rex chirps stacked in the time domain at the source location of −5 m, as derived from the

We show evidence that short wavelength DAS dispersion measurements are limited near and below the acquisition gauge length. These observations make gauge length selection an important factor to consider in future near-surface studies using DAS. Vantassel et al. (2022)

# MASW: Geophones vs. DAS – dispersion data

“The experimental dispersion data (mean +/− one standard deviation range) recovered from the geophone and DAS systems show excellent agreement for all three recovered Rayleigh modes.”

“When appropriate considerations are made to ensure proper cable selection, good cable-soil coupling, and sufficiently short gauge lengths, DAS can be an effective alternative to geophones for the purpose of acquiring dynamic signals for the intent of extracting high-resolution, multi-mode surface wave dispersion using the MASW technique.”

Vantassel et al. (2022)

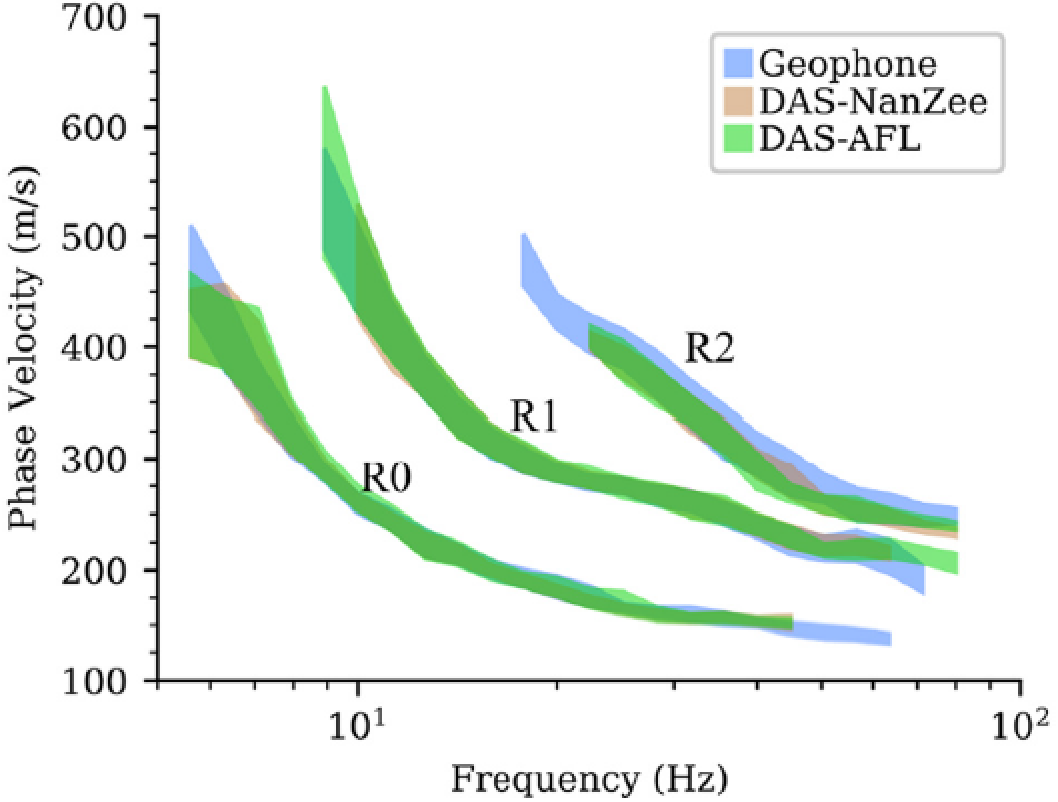

**Fig. 10.** Comparison between the geophone-derived and DAS-derived (NanZee and AFL) experimental dispersion data at the Hornsby Bend site. The vertical range at each frequency represent the mean +/− one standard deviation of the experimental dispersion data for the fundamental, first-higher, and second-higher Rayleigh modes (R0, R1, and R2, respectively).

# MASW: 1D Vs Inversions from Mulit-mode DAS Dispersion Data

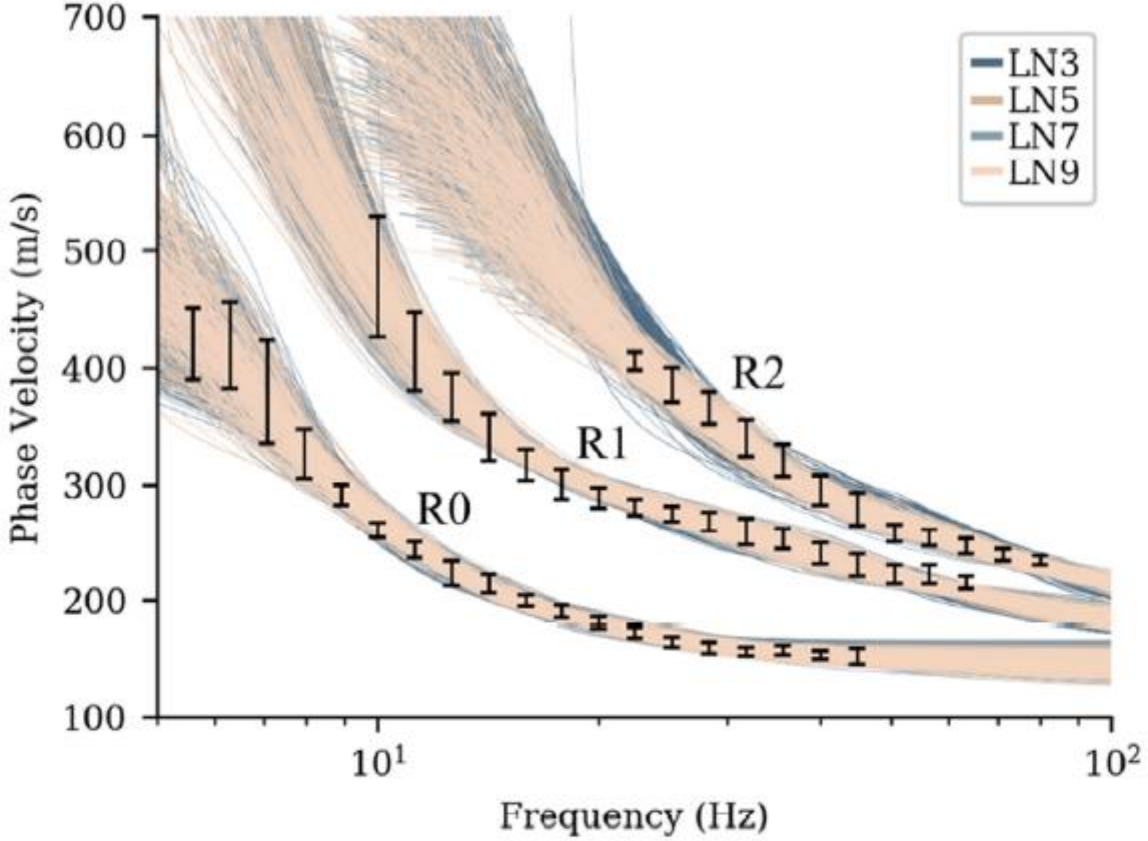

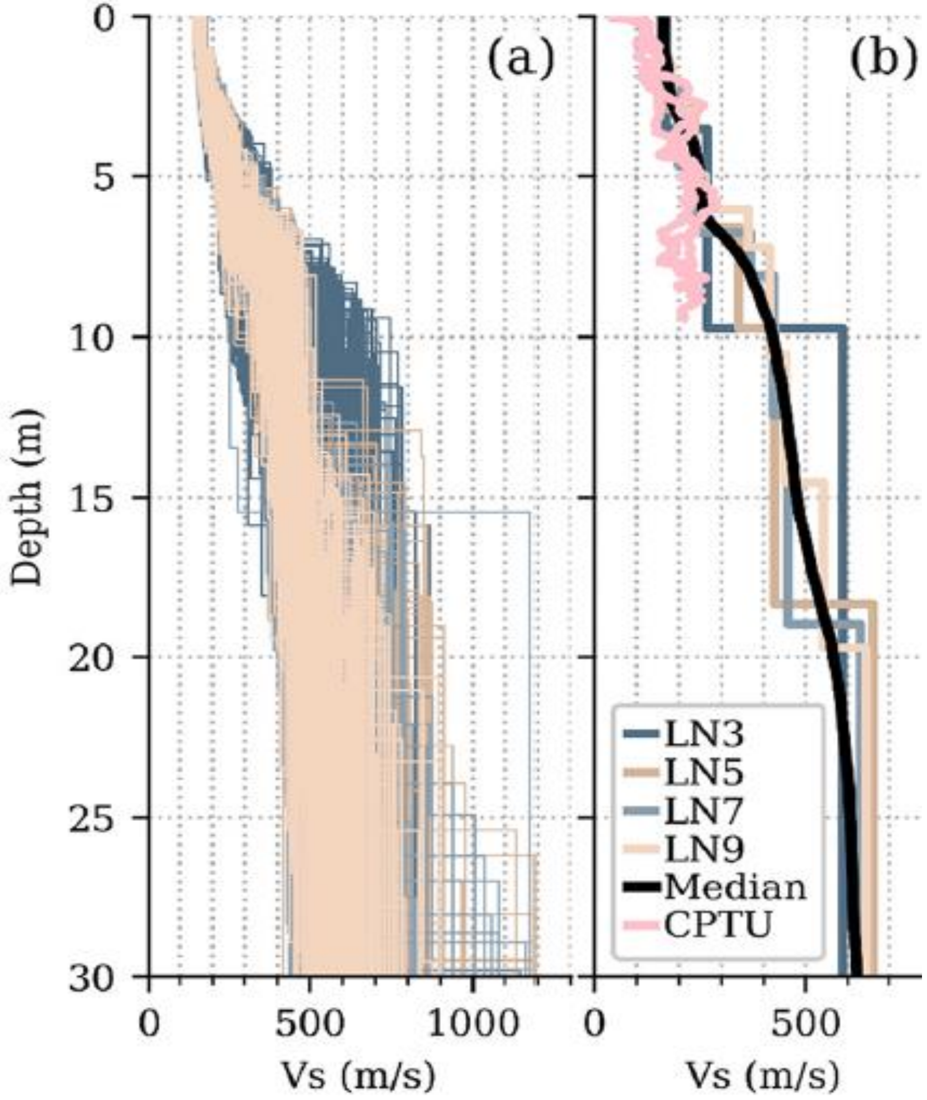

# DAS Pseudo-2D MASW at Hornsby Bend

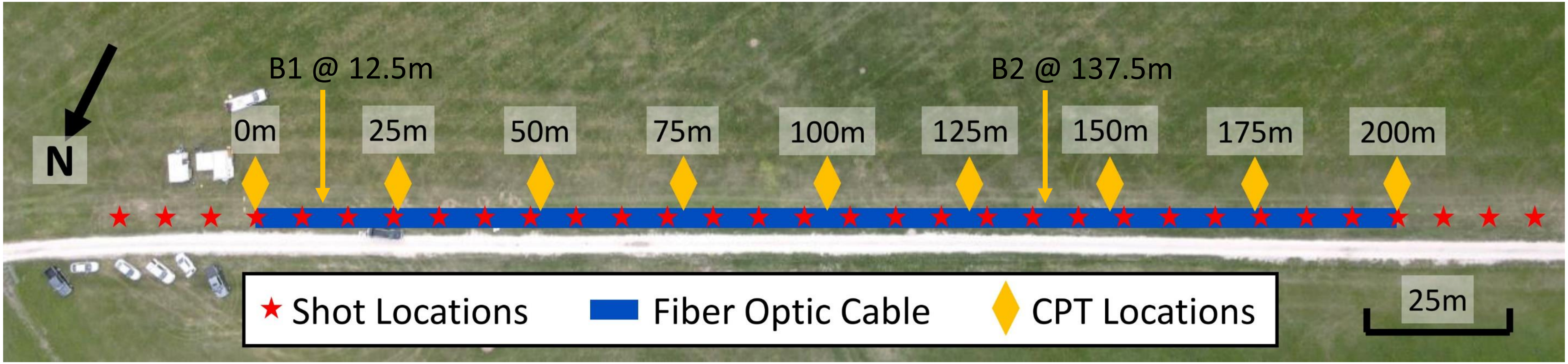

- 200-m long DAS array consisting of 196 channels
  - 1.02-m channel spacing, 2.04-m gauge length
- 32 shot locations using Thumper every 8m from -24m to 224m
  - Vertical sweep from 5 Hz to 200 Hz linearly with 0.5-s cosine taper
- 9 CPT soundings taken every 25m
- Two boreholes, B1 and B2, were drilled at 12.5m and 137.5m
  - Downhole testing performed in B1

# DAS Allows for Flexible Sub-Array Geometry

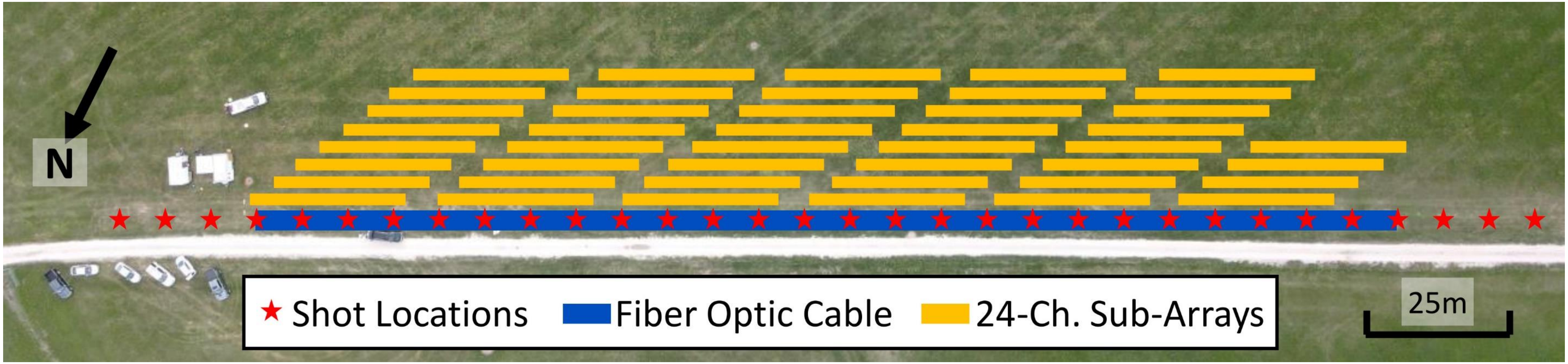

- 47 12-channel sub-arrays
- 44 24-channel sub-arrays (shown above)
- 38 48-channel sub-arrays

# Dispersion Data: Impact of Sub-Array Length

- Consistent $\lambda_{min,avg}$
  - – 6.4 m to 6.6 m
- Varying $\lambda_{max,avg}$
  - – 12-channels: 20 m
  - – 24-channels: 28 m
  - – 48-channels: 39 m
- Shorter arrays slightly more variable within shared range.

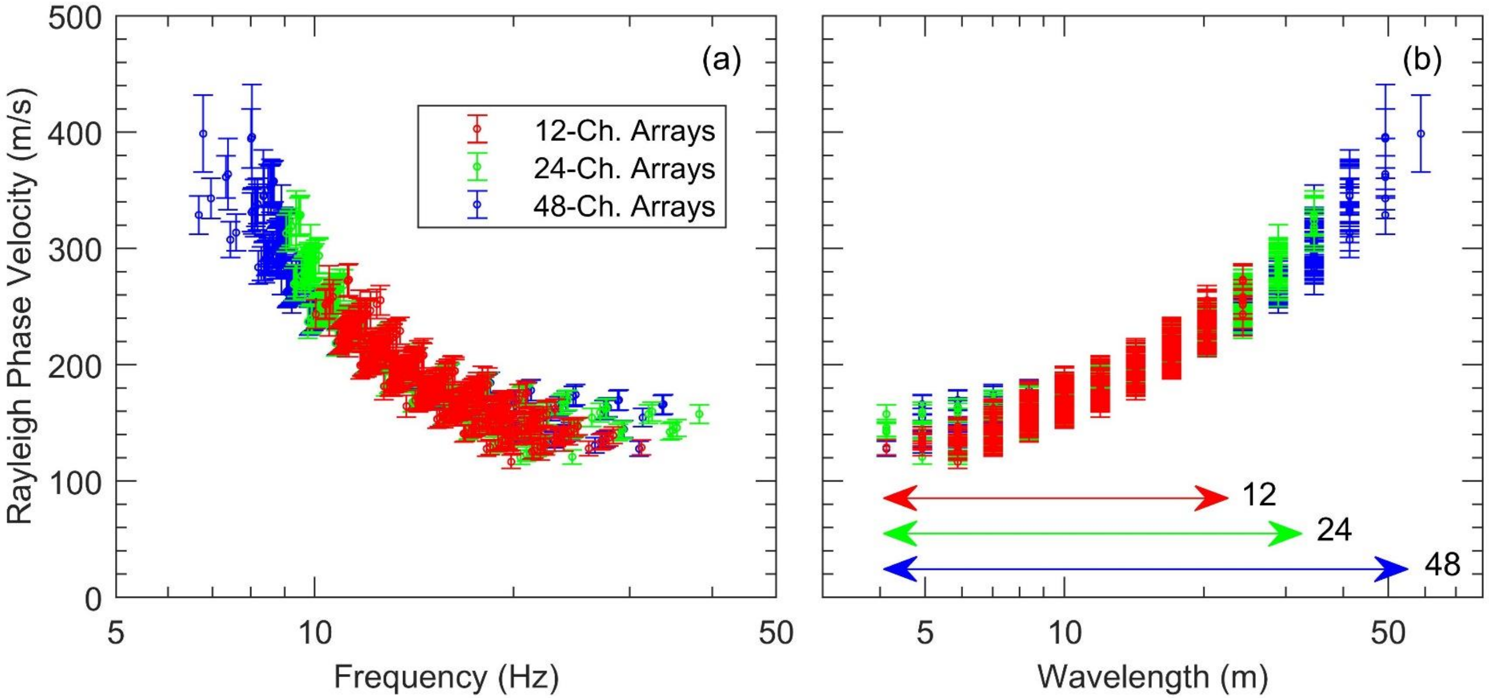

# Pseudo-2D Vs Cross Sections: Impact of Sub-Array Length

- Two boreholes drilled along the DAS array
  - B1 at 12.5 m
  - B2 at 137.5 m
- Downhole testing performed in B1
- Different cross-sections agree best with different invasive test results

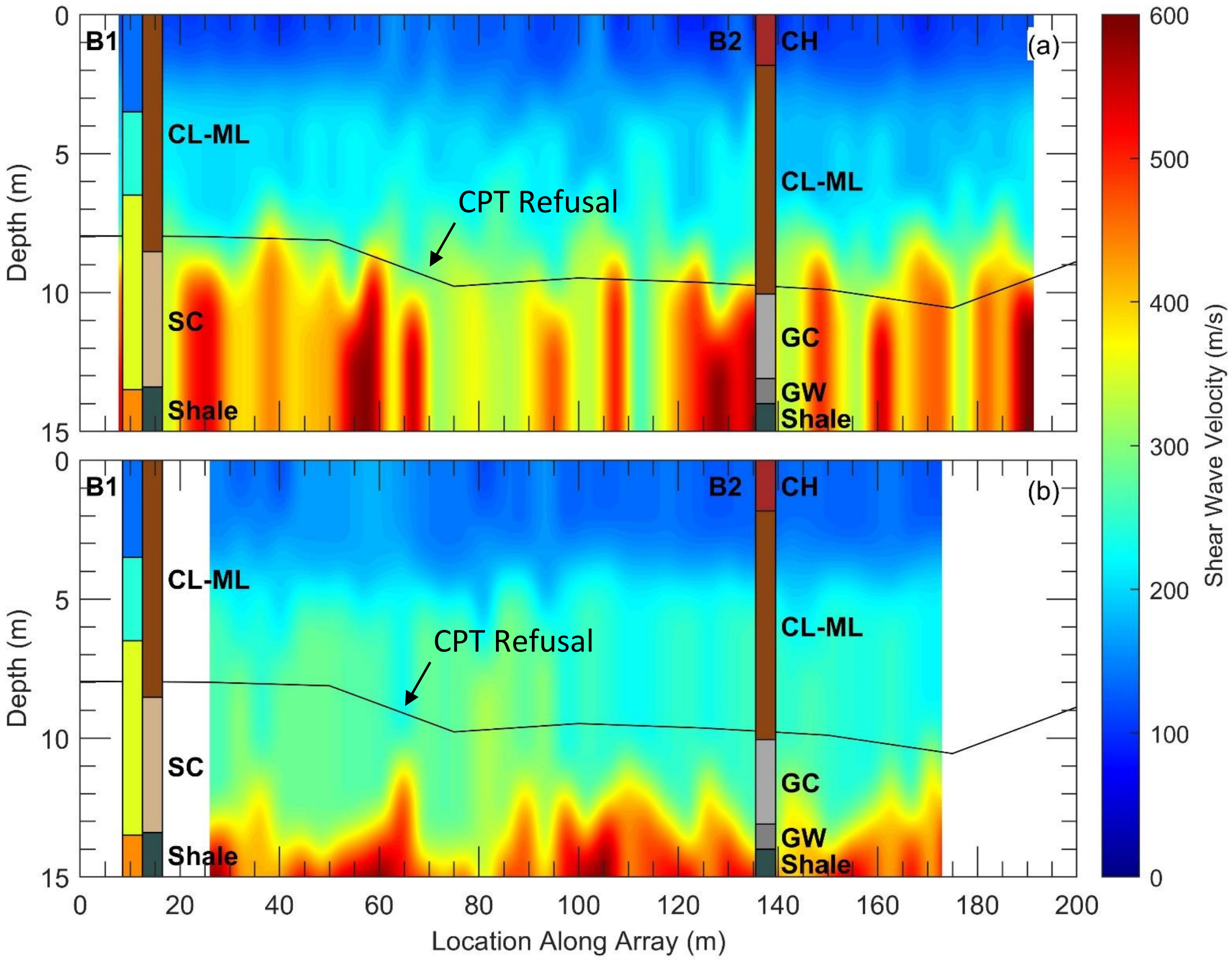

12 Ch.

48 Ch.

# DAS 2D Imaging via FWI at Hornsby Bend

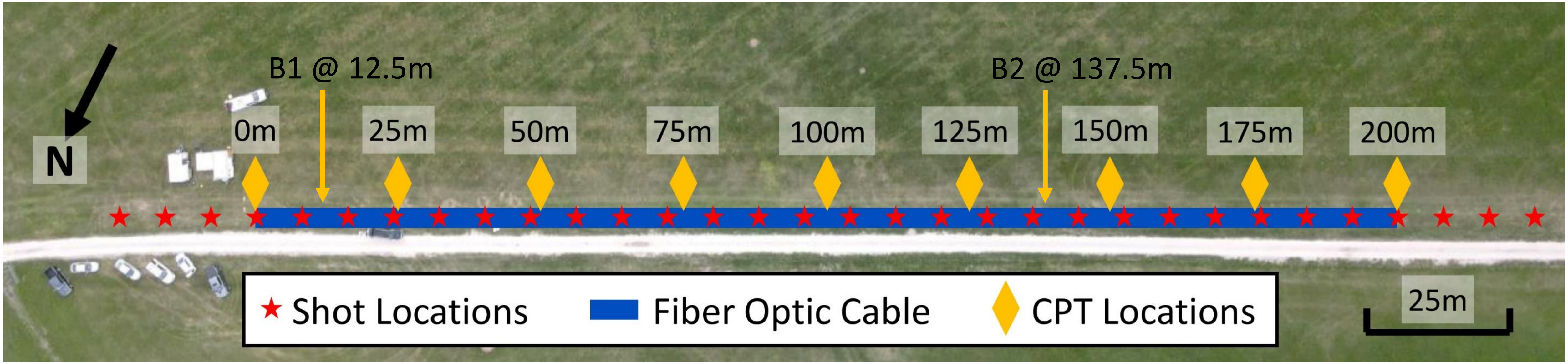

- 200-m long DAS array consisting of 196 channels
  - 1.02-m channel spacing, 2.04-m gauge length
- 32 shot locations using Thumper every 8m from -24m to 224m
  - Vertical sweep from 5 Hz to 200 Hz linearly with 0.5-s cosine taper
- 9 CPT soundings taken every 25m
- Two boreholes, B1 and B2, were drilled at 12.5m and 137.5m
  - Downhole testing performed in B1

# DAS FWI Using Salvus Software

- The Salvus software package by Mondaic AG was used to process the raw data and perform the inversions
  - The spectral-element method is used to perform simulations (Afanasiev et al. 2019)
  - The elastic wave equation is derived in terms of displacement (*u*)

© Mondaic AG

$$\rho(x)\partial_t^2 u(x,t) - \nabla \cdot \left(C(x){:}\,\varepsilon(u)(x,t)\right) = f(x,t)$$

Misfit also in terms of $u$: $\chi(u)$ Derived field: $q = q(u) = \mathcal{D}u = e^T \varepsilon(u) e$

  - Adjoint strain sources are implemented as moment tensor sources rather than the vector sources used for velocity (geophone) data

$$\left(\mathcal{D}^\dagger \frac{\partial}{\partial q}\chi, \delta u\right) = \left(\frac{\partial}{\partial q}\chi, \mathcal{D}(\delta u)\right) = \left(\left(\frac{\partial}{\partial q}\chi\right) e e^T, \varepsilon(\delta u)\right)$$

Vector Source Tensor Source

Tensor Source

# Stage 1 (10 to 15 Hz) - Shot 1 - Observed Data

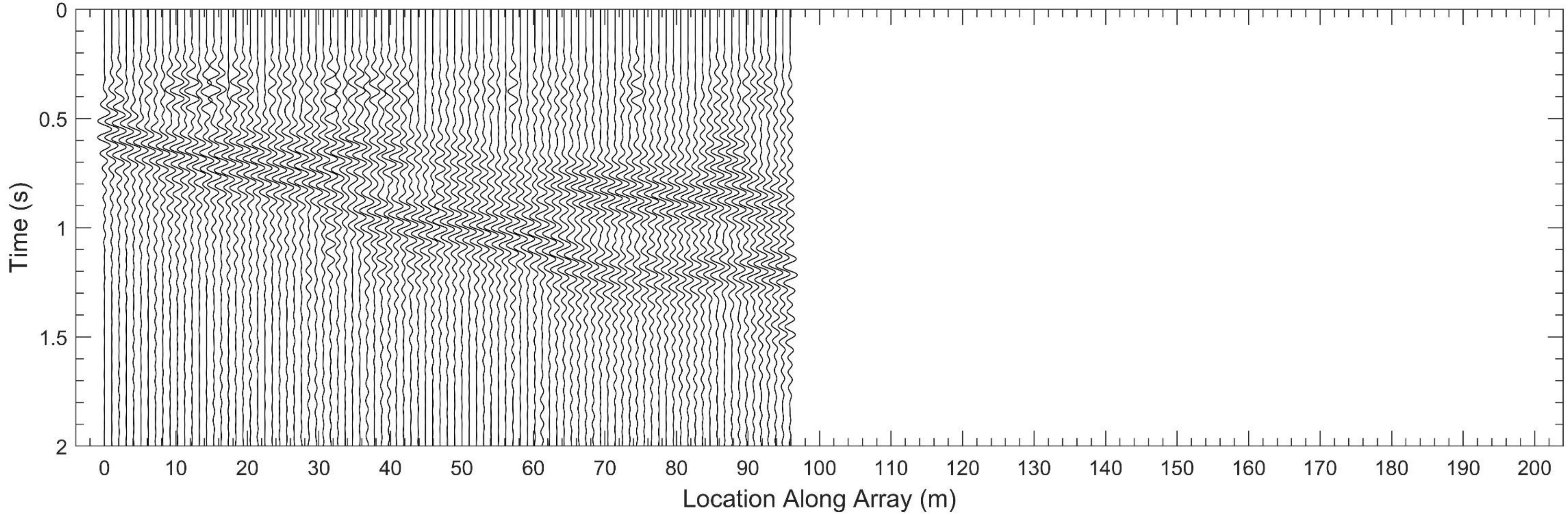

- The observed waveforms are correlated with the Thumper’s ground force output
- A point-to-line source conversion is applied (Forbriger et al. 2014)
- Only channels 20 m to 120 m away from each shot location are inverted

# Stage 1 (10 to 15 Hz) - Shot 16 - Observed Data

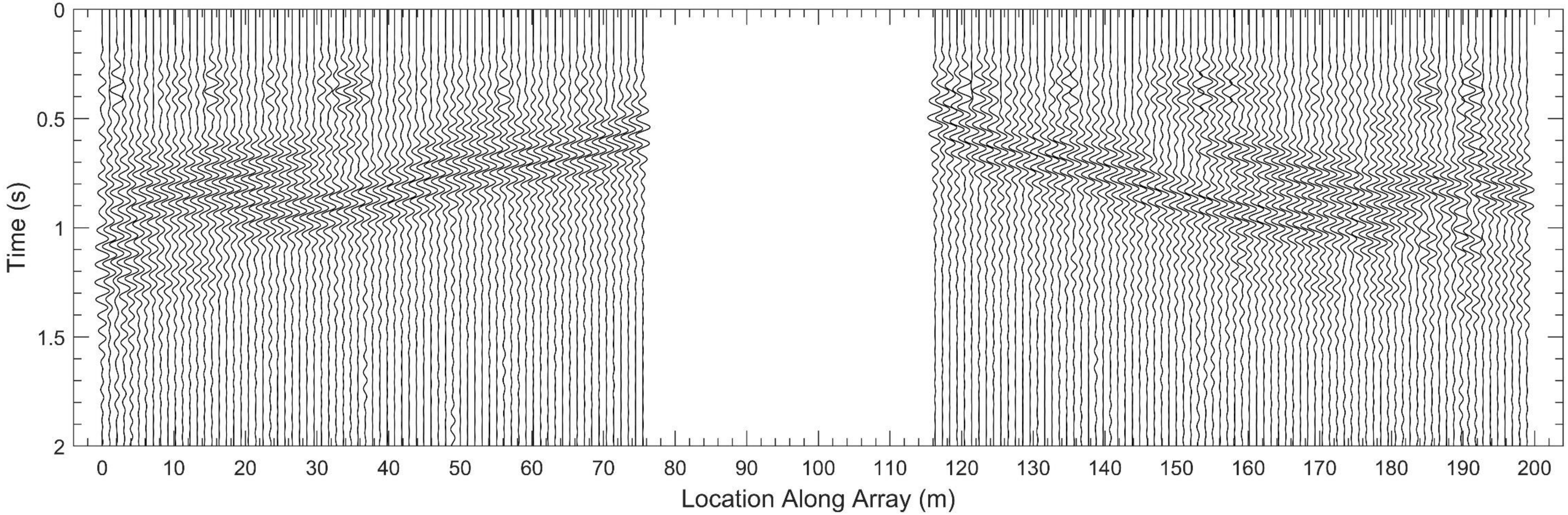

- The observed waveforms are correlated with the Thumper’s ground force output
- A point-to-line source conversion is applied (Forbriger et al. 2014)
- Only channels 20 m to 120 m away from each shot location are inverted

# Stage 1 (10 to 15 Hz) - Shot 32 - Observed Data

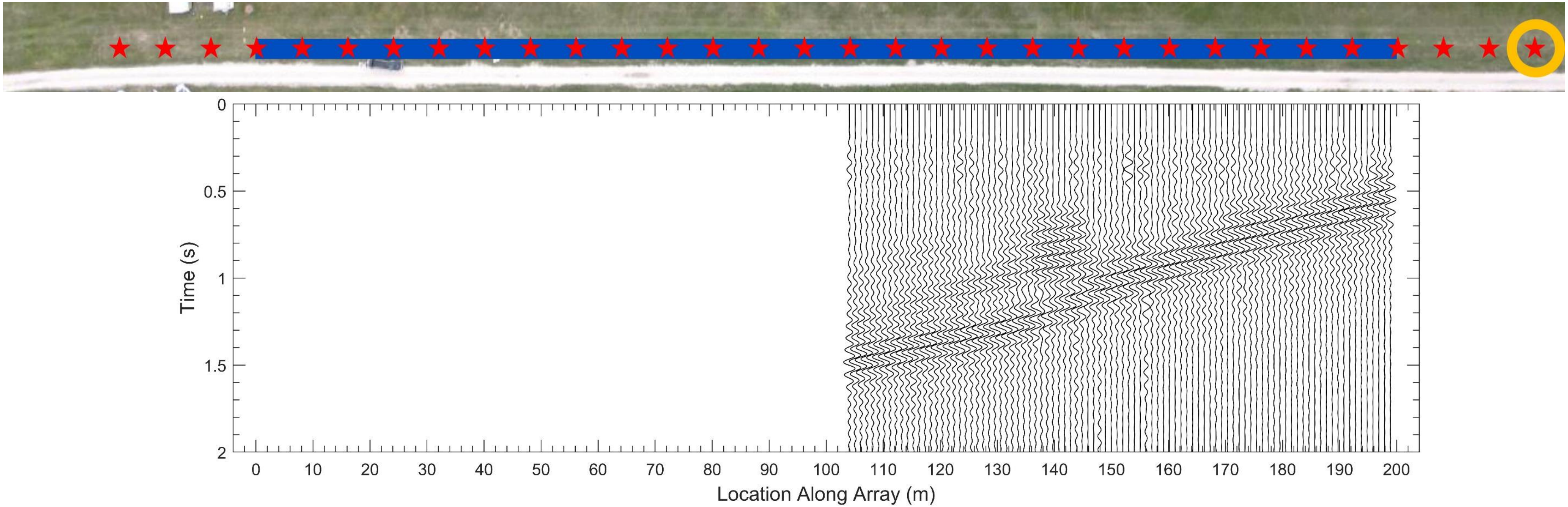

- The observed waveforms are correlated with the Thumper’s ground force output
- A point-to-line source conversion is applied (Forbriger et al. 2014)
- Only channels 20 m to 120 m away from each shot location are inverted

# Investigated 4 Different Starting Models for FWI

- Each model has five parameters
  - $V_S$ based on test results
  - $V_P=2V_S$ for all but DH
  - $\rho = 1000(0.31\ V_P^{0.25})$ (Gardner et al.1974)
  - $Q_\mu = 100$ and $Q_\kappa = 15$ based on amplitude decay of far offset channels

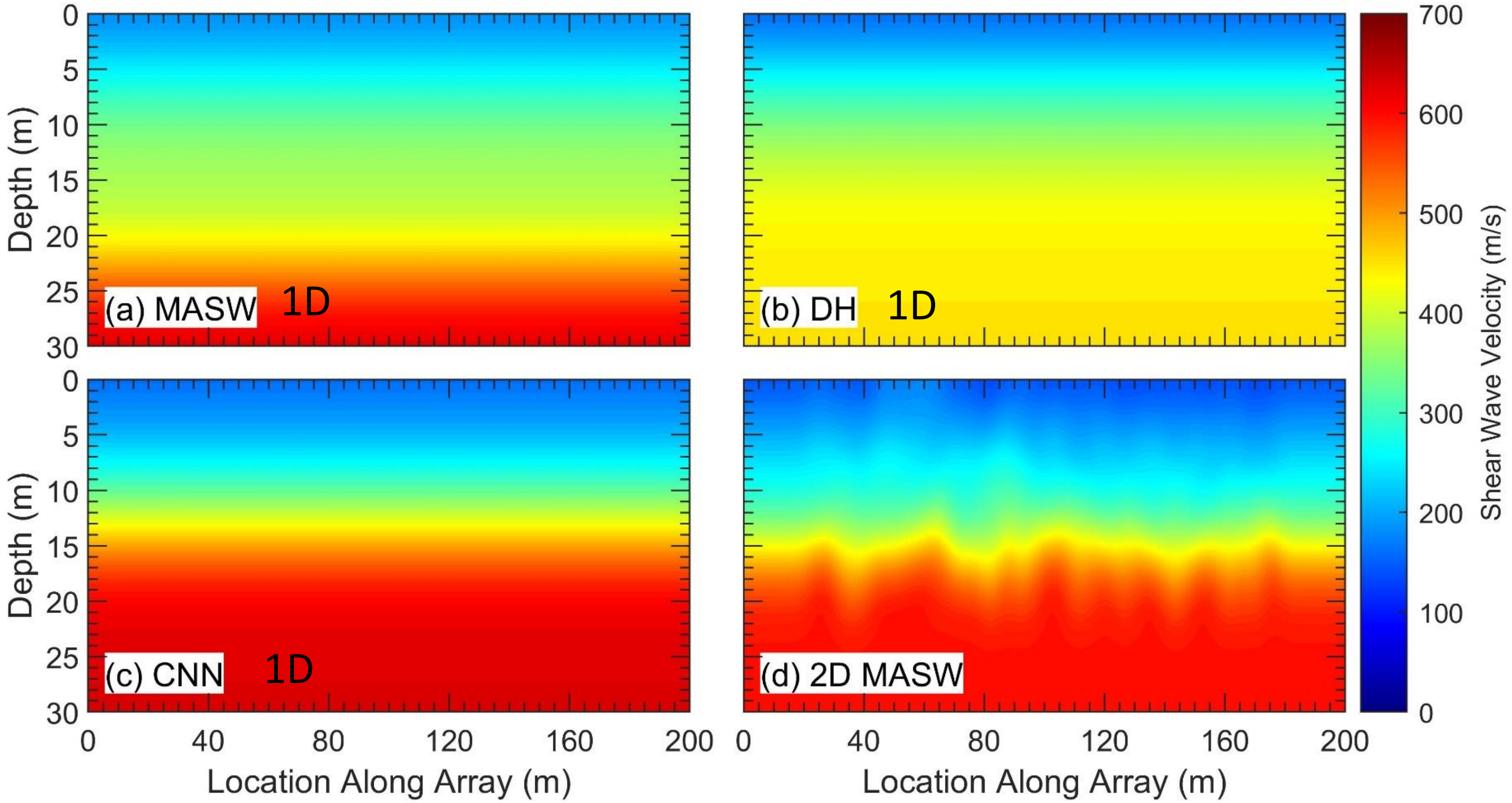

# Stage 1 (10 to 15 Hz) – 1D MASW Model Update

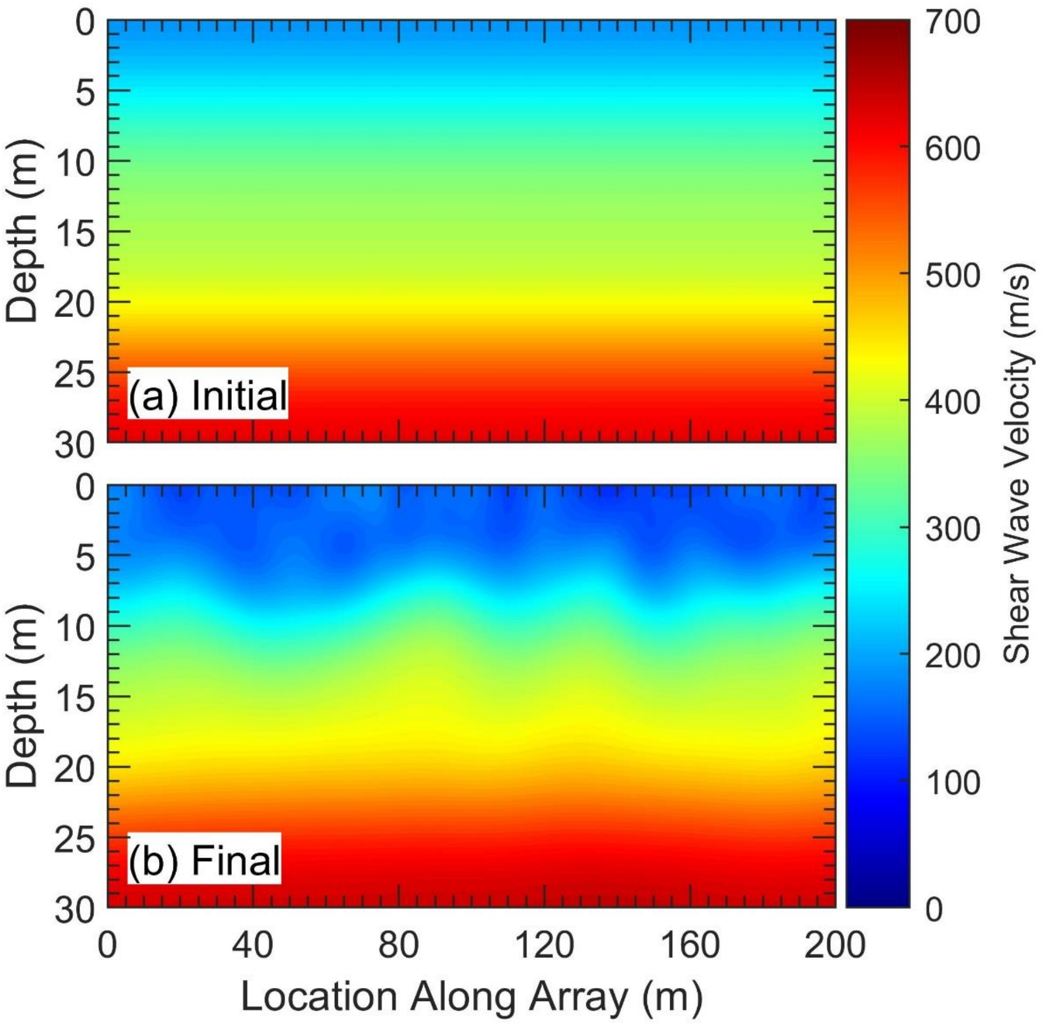

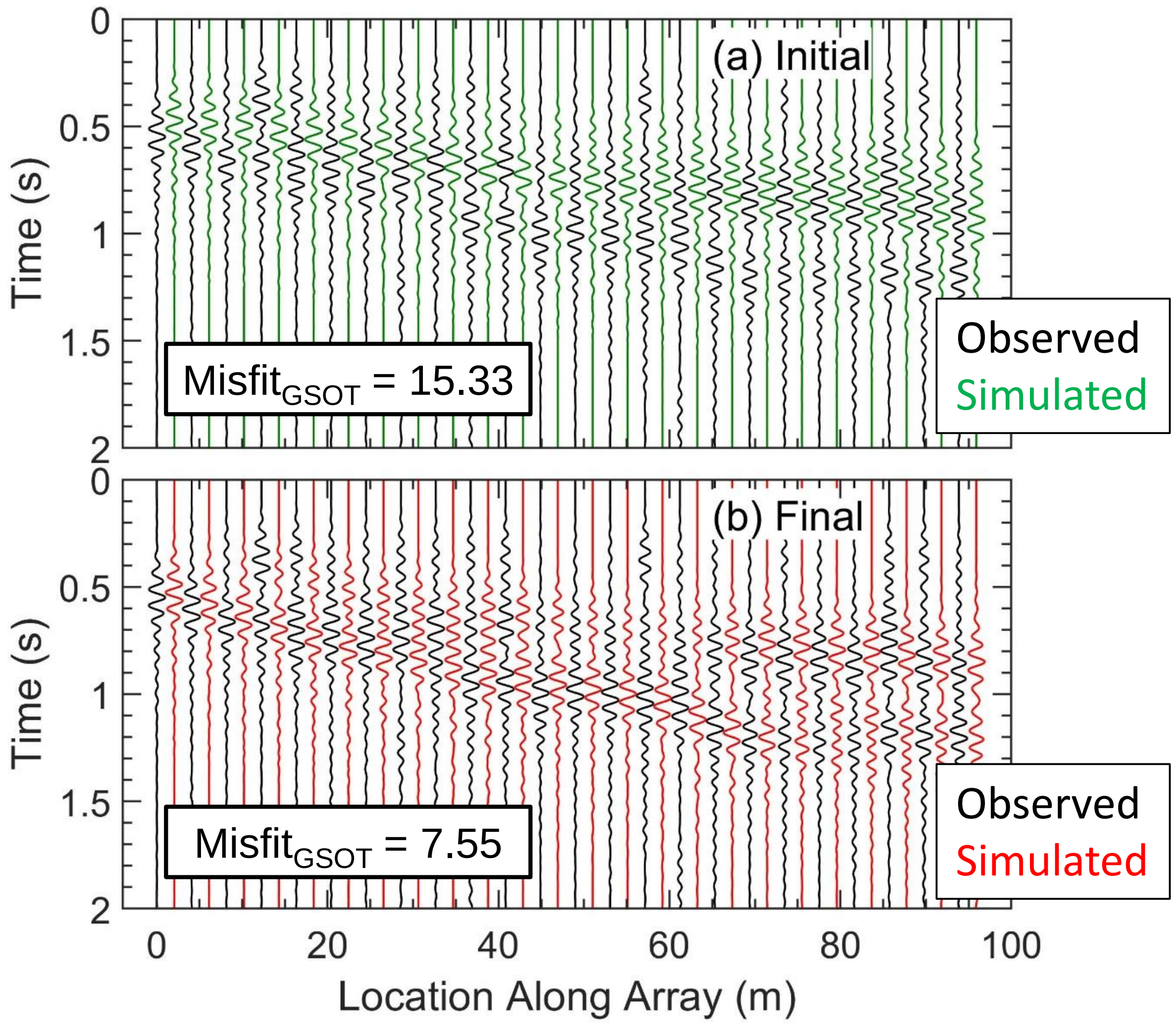

# Evolution of VS in the 1D MASW Model

- Majority of the changes occur in Stage 1
- Higher-frequency data in later stages corresponds to smaller features
- Simulations are more costly as the stages progress

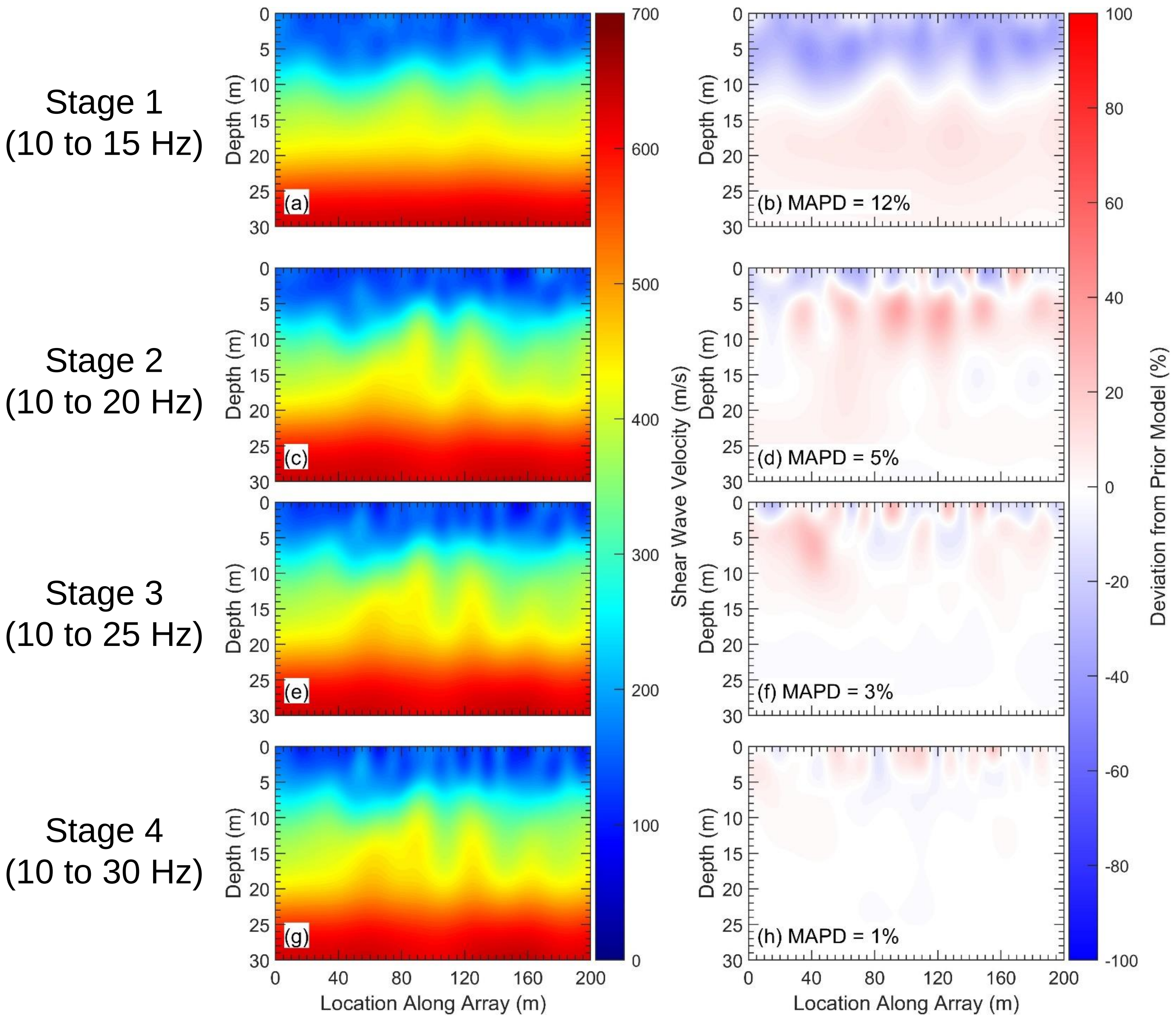

# Stage 4 (10 to 30 Hz) Final Models: Observed vs. Simulated Waveforms

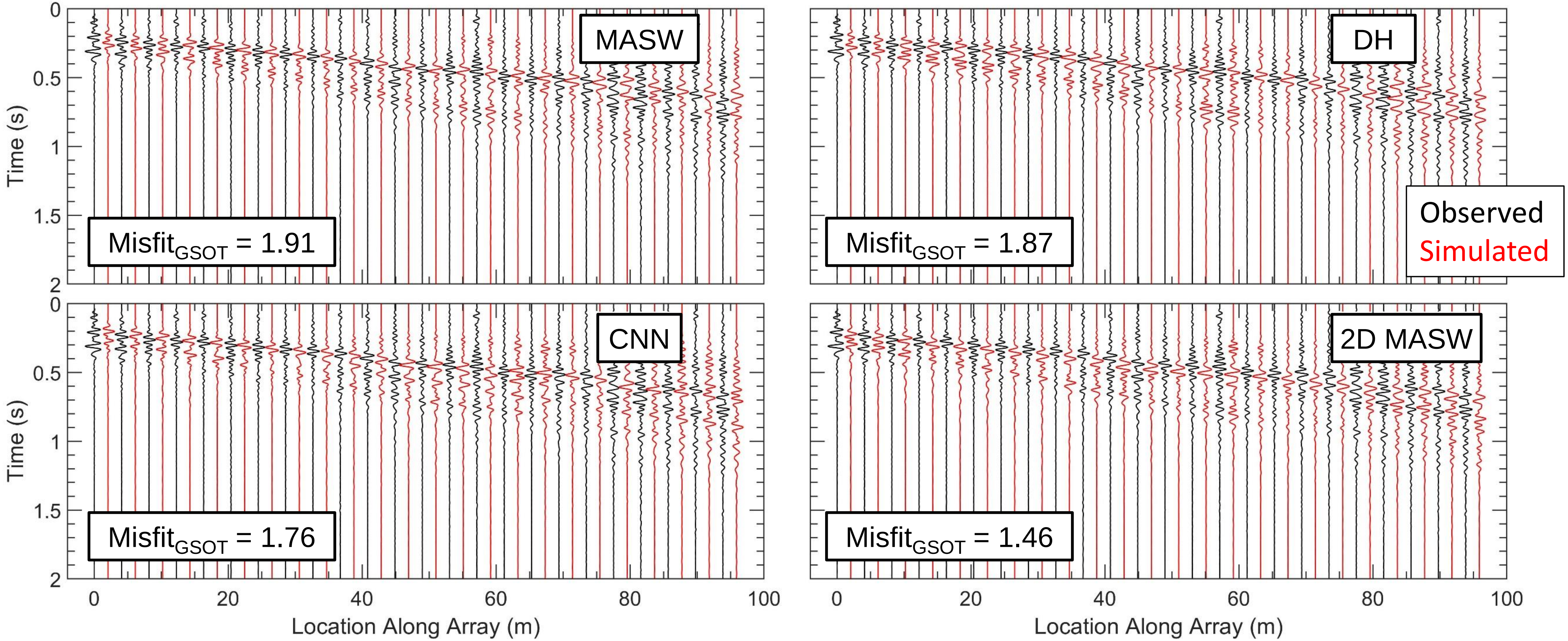

# Comparison of Final 2D Vs Images with Invasive Testing Data

- Despite very similar waveform misfits, the final 2D Vs images are quite different, highlighting non-unique nature of FWI
- All starting models yield quite similar Vs images over top ~ 10m
- The CNN and 2D MASW starting models seem to produce results that are most consistent with the invasive data

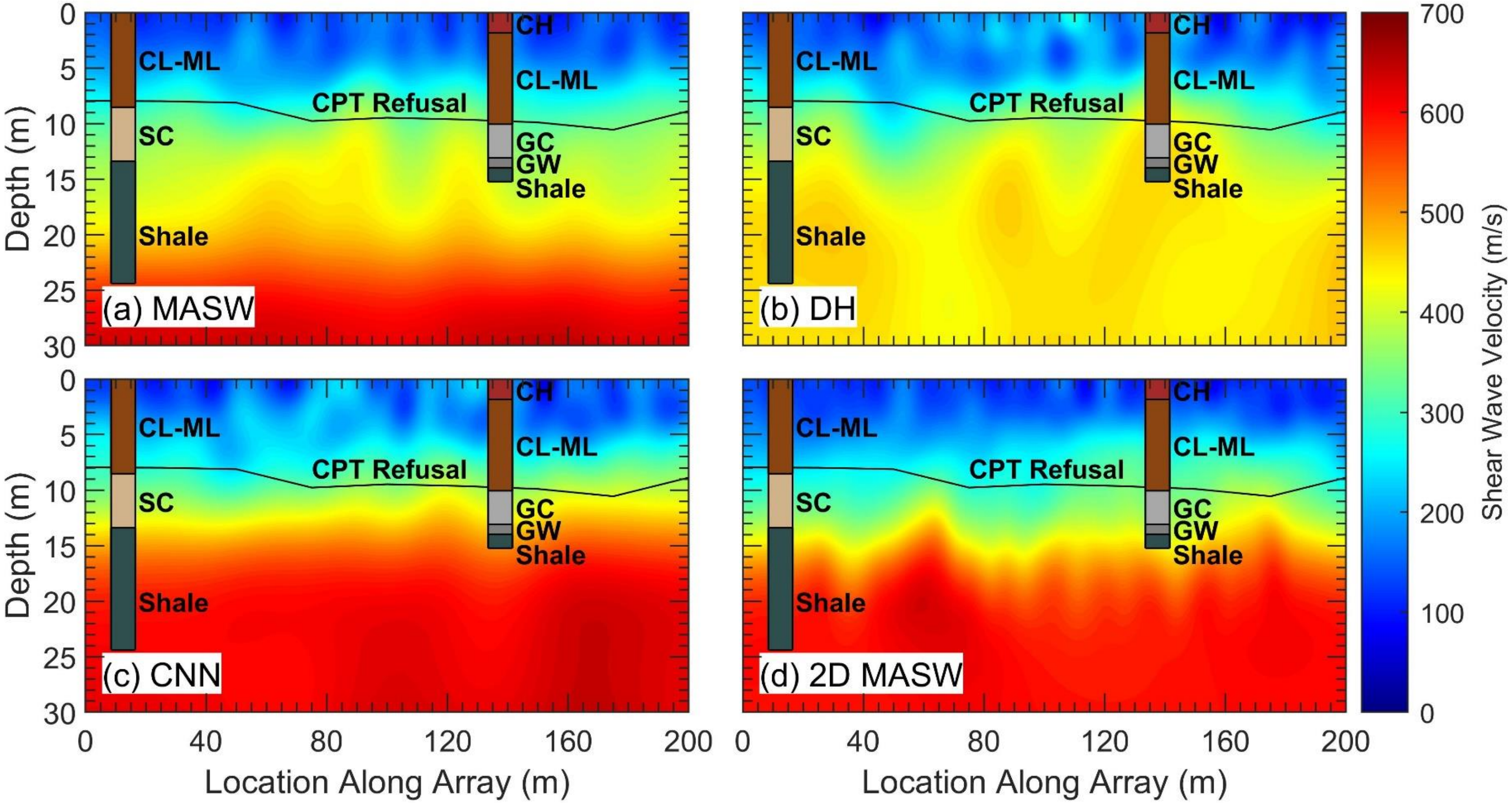

# DAS for 3D Imaging at the Newberry, FL Site

https://youtu.be/BrEPCvoeiiE



Public Dataset will be Published Soon


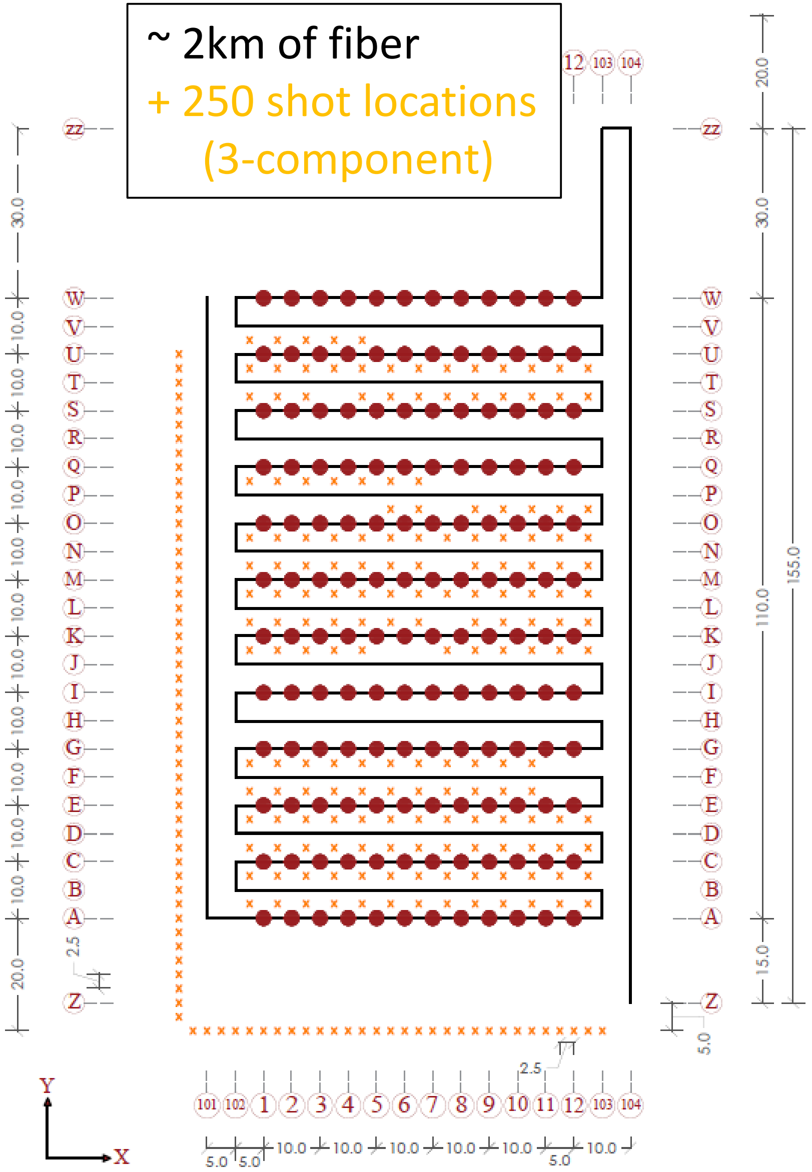

~ 2km of fiber
+ 250 shot locations
(3-component)

# Conclusions

- The 1D nature of DAS (i.e., axial strain) makes its reception to seismic waves complicated.
- The theory of DAS reception can be used along with controllable source polarizations to create optimal configurations for the application of interest.
- NHERI@UTexas's seismic shakers are capable of generating vertical and 2-component horizontal shaking that can be used for a variety of DAS imaging applications.
- More research needs to be done to show how active-source surface seismic experiments can leverage the directionality of both sources and sensors to improve seismic imaging.

# We Look Forward to Supporting Your DAS Research with our NHERI@UTexas Shakers and DAS IU

# Questions?

LARGE MOBILE SHAKERS

NHERI@UTexas